

1. JSC «PKK Milander» Microcircuit 1986VE8T. Specification. Version 2.5.0 of
12.12.2015

REMOVING THE INFLUENCE OF NONLINEAR DISTORTIONS IN THE METHODS USING PHASE SHIFT INTERFEROMETRY

Guzhov V.I., Ilinykh S.P.

Novosibirsk State Technical University, Novosibirsk Russia
+7 (913) 925-39-24, vigguzhov@gmail.com

Abstract—The proposed method for analyzing 3D images is not sensitive to the distortion of the profile of the projected interference fringes. The implementation of the method involves obtaining a series of images with different phase shifts.

Keywords — gamma distortion; non-contact measurements; Fourier transform, phase shift.

INTRODUCTION

The Structured Light Interferometry method (SLI) is a triangulation method based on a three-dimensional (3-D) method for reconstructing the surface of a measured object [1]. The method is based on measuring the distortion of interference fringes in proportion to the profile of the surface relief, when they are observed at an angle to the projector. Figure 1 shows the principle of measuring the height profile.

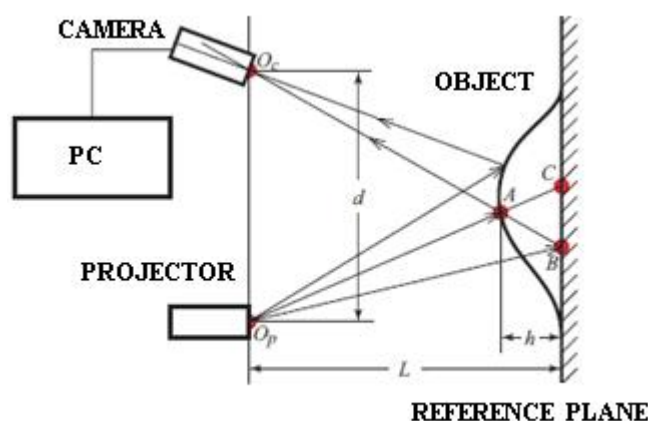


Fig. 1. Projection method for measuring the relief.

The intensity recorded by the camera can be represented as follows

$$I_c(x, y) = \alpha(x, y) \left(A_c + B_c \cos(2\pi f_\varphi y + \varphi(x, y)) \right), \quad (1)$$

where (x, y) image coordinates and $\alpha(x, y)$ surface reflection coefficient, A_c and B_c average brightness and amplitude of the bands, f_φ - frequency of the projected sinusoidal array, $\varphi(x, y)$ the profile depth of the sinusoidal grid is proportional to the depth of the relief or the interference pattern of the phase [2]. The method allows to directly measuring the spatial coordinates of the relief of an object commensurable with the period of the projected lattice. As shown in Fig. 1, the height of the relief is described by the following

$$h = BC \cdot (L / (1 + BC/D) D), \quad (2)$$

where $BC = \beta(\varphi_A - \varphi_B + 2\pi N)$, β - geometric parameter, $\varphi_A - \varphi_B = \varphi$ - phase difference in points A and B, φ - local phase corresponding to the fractional part of the phase of the general phase $\Phi(x, y)$. To calculate the phase, the phase shift method [2] is used, in which a set of interferograms with different phase shifts is recorded:

$$I_i(x, y) = \alpha(x, y) (A + B \cos(\varphi(x, y) + \delta\varphi_i)). \quad (3)$$

The phase shift $\delta\varphi$ is formed by the spatial displacement of the image in proportion to the period of the sinusoidal bands T. The shift $\delta\varphi$ of the grating for one period is equivalent to a phase shift equal to $\delta\varphi_0 = 0$, $\delta\varphi_1 = 2\pi/3$ and $\delta\varphi_2 = 4\pi/3$. For example, when the phase shifts are equal, and we get the following decoding formula

$$\varphi = \arctan[(I_3 - I_2) / (3I_3 - 3I_2)]. \quad (4)$$

The accuracy of this method depends on the profile of the projected bands, which usually has a sinusoidal shape. Gamma distortions [2] make the ideal sinusoidal waveform non-sinusoidal, as shown in Fig. 2 (top), so that as a result, their phase is distorted. Figure 1 (bottom) shows the shape of the distorted sinusoid in the frequency domain, where the highest pulse is the DC component, while the second highest pulse is the amplitude of the first harmonic, which is a component of the phase and is used in profilometry [3]

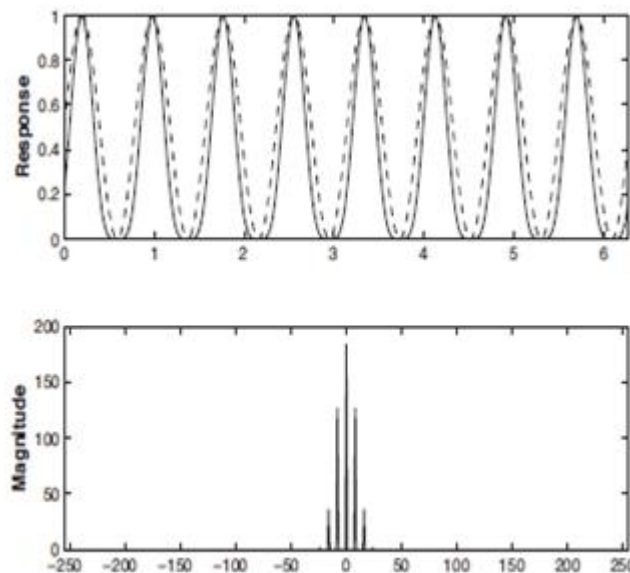


Fig. 2. Ideal and distorted ($\gamma = 2.2$) sinusoidal wave (top), and the amplitude of the distorted sinusoidal wave in the frequency domain (bottom).

Under ideal conditions, the first-order harmonic is the only nonzero component in the Fourier domain, but if gamma distortions are present, higher-order harmonics appear [4]. To eliminate this effect, two approaches are used. In the first approach, it is assumed that the projected image is precompensated to the object by changing the hardware illumination table in

the projector (LUT) [5]. The accuracy of the phase compensation depends on the length of the LUT, since the measured data phase is related to interpolation in real time. Another approach is based on the use of gamma-ray model, which allows you to analytically describe the images perceived by the camera [6]. In addition, this problem is relevant both for structured radiation methods and for other measurement technologies using step-by-step phase shift [7-10]. The proposed algorithm of interferograms analysis allows eliminating the influence of gamma distortion on the measurement results.

PROBLEM STATEMENT

Taking into account gamma distortions, the intensity of the recorded image at the point is defined as [10]

$$I_i^\gamma(x, y) = [\alpha(x, y)(A + B \cos(\varphi(x, y) + \delta\varphi_i))]^\gamma, \quad (5)$$

where γ - ratio of gamma distortion..the ratio of gamma distortion.

The non-linear characteristics (5) is usually approximated by a polynomial of n - degree

$$I^\gamma = a_0 + a_1 I + a_2 I^2 + a_3 I^3 + \dots + a_{n-1} I^{n-1} + a_n I^n. \quad (6)$$

Figure 3 shows a change in the interference band profile for gamma distortion.

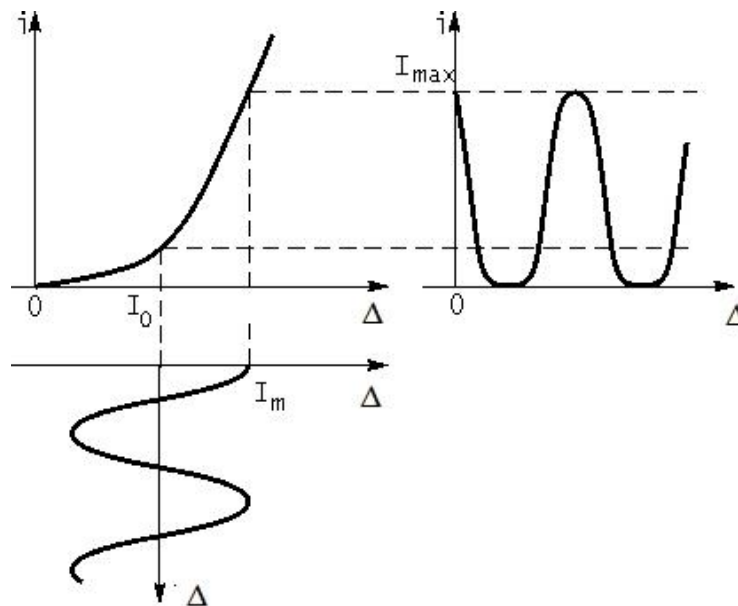


Fig. 3. The transform of harmonic signal by nonlinear characteristics.

Substituting in (6) intensity expression (3) and performing trigonometric transformations we obtain

$$I^\gamma = I_0 + I_1 \cos(\varphi + \Delta_1) + I_2 \cos(2\varphi + 2\Delta_2) + \dots + I_n \cos(n\varphi + n\Delta_n). \quad (7)$$

The expression (7) is a Fourier transform of the original sequence (5). Thus, the transform of harmonic signal by nonlinear characteristics of the resulting spectrum, the highest harmonic which is equal to the degree of the polynomial. It should be noted that the number of harmonics in this case is equal to the number of phase shifts in (3). The initial phase of the harmonics are related by

$$\varphi_k = k\varphi \text{ и } \varphi = \varphi_k / k . \quad (8)$$

here k – harmonic number.

For a number of reasons, the direct application of the Fourier transform to calculate the first harmonic does not allow for high measurement accuracy. For example, the limitation of the spectrum and not multiplicity of the signal period leads to the appearance of Gibbs effect, which leads to the "plugging" of harmonics and, accordingly, to their distortion.

The aim of the work is to build an algorithm to avoid the use of Fourier transform in the calculation of the complex amplitude of the first harmonic.

SOLUTION OF THE PROBLEM

The main idea of the work is the choice of phase shifts, in which the influence of higher harmonics will be minimized. Figure 4 shows the phase shifts in which the effect of the third harmonic is minimized. Similarly, you can pick up phase shifts for other harmonics.

The study of the dependence of the number of harmonics on the value of the gamma distortion coefficient showed that if it is within 1-8, it is enough to take into account the first four harmonics. This condition corresponds to phase shifts $\delta\varphi_0 = 0$ and $\delta\varphi_1 = \pi$ - these phase shifts are compensated even harmonics. Phase shifts $\delta\varphi_2 = \pi/3$ and $\delta\varphi_3 = 5\pi/3$ compensates for the third harmonic.

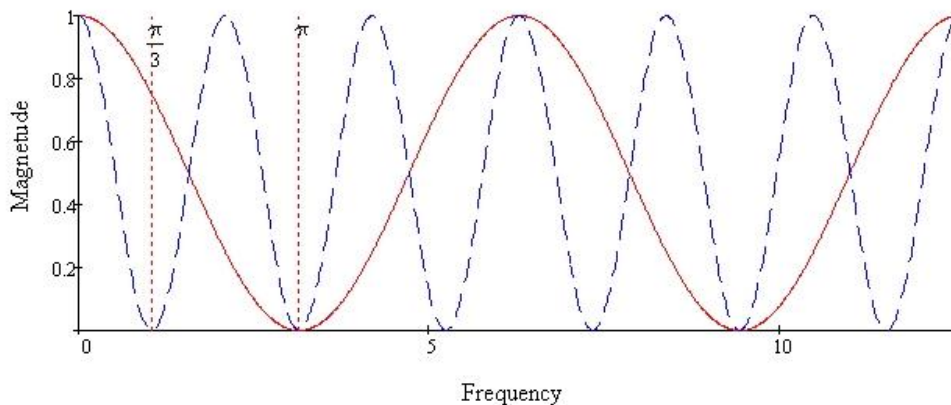


Fig. 4 Phase shifts minimizing the influence of the third harmonic..

Substituting these phase shifts into expression (3), we obtain the following sequence of interferograms

$$I_1 = A + B \cos(\varphi + \delta\varphi_0), \quad I_2 = A + B \cos(\varphi + \delta\varphi_1), \quad I_3 = A + B \cos(\varphi + \delta\varphi_2) \text{ и } I_4 = A + B \cos(\varphi + \delta\varphi_3) . \quad (9)$$

Combining interferograms (9) it is possible to obtain an expression defining the real part of the complex value of the first harmonic coefficients $z_1 = a_1 + ib_1 = B \cos(\varphi) + iB \sin(\varphi)$, $i = \sqrt{-1}$

$$G_1 = A + B \cos(\varphi) = I_1 + 1/2(I_1 - I_2) + 1/3(I_3 - I_2) + 1/3(I_4 - I_2) . \quad (10)$$

To eliminate the constant component, it is necessary to form a similar sequence with a shift by half of the signal period and subtract it from the previously obtained harmonic value. This corresponds to phase shifts $\delta\varphi_4 = \pi$, $\delta\varphi_5 = 2\pi$. Phase shifts $\delta\varphi_6 = 4\pi/3$ and $\delta\varphi_7 = 2\pi/3$ compensates for the third harmonic.

$$G_2 = A - B \cos(\varphi) = I_5 + 1/2(I_5 - I_6) + 1/3(I_7 - I_6) + 1/3(I_8 - I_6) \quad (11)$$

Then

$$\therefore G = B \cos(\varphi) = 1/2(G_1 - G_2) \quad (12)$$

Substituting expressions (9) and (10) into the expression (11) we finally obtain

$$G = 1/6(3I_1 - I_2 + 2I_3 + 2I_4 - 3I_5 + I_6 - 2I_7 - 2I_8) \quad (13)$$

Similarly, you can get an expression for $B \sin(\varphi)$. To do this, taking into account the known trigonometric equality $\sin(\varphi) = \cos(\varphi + \pi/2)$, it is necessary to shift all phase shifts by an equal value $\pi/2$, i.e. $\delta\varphi_i = \delta\varphi_i + \pi/2$, to perform transformations (9) – (13) again. Thus, we obtain the formula for decoding interferograms

$$\tan(\varphi) = \frac{B \sin(\varphi)}{B \cos(\varphi)} = \frac{3I_9 - I_{10} + 2(I_{11} + I_{12}) - 3I_{13} + I_{14} - 2(I_{15} + 2I_{16})}{3I_1 - I_2 + 2(I_3 + I_4) - 3I_5 + I_6 - (2I_7 + I_8)} \quad (14)$$

Note that some of the phase shifts in the numerator and denominator have the same values, i.e. in our case it is necessary to make not 16, but 12 phase shifts.

To test the developed algorithm, the phase is calculated by four-point algorithm (4), eleven-point algorithm with phase shifts multiple $\pi/2$ [11]

$$\tan(\varphi) = \frac{(I_1 - I_{11}) - 8(I_3 - I_9) + 15(I_5 - I_7)}{(4I_2 - I_{10}) + 12(I_4 - I_8) + 16I_6} \quad (15)$$

and according to the proposed algorithm. The results of the calculations are shown in figures 5 and 6. Figure 5 shows the phase values. Here-a solid thin line corresponds to the algorithm (4), a solid bold line corresponds to the algorithm (15), and a dashed line corresponds to the proposed algorithm (14).

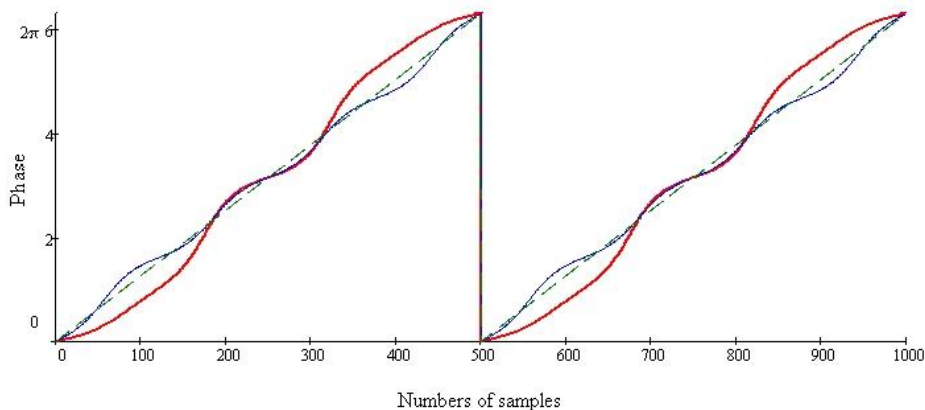


Fig. 5. Comparison of algorithms (4), (14) and (15)

Figure 6 shows the errors of each of these methods.

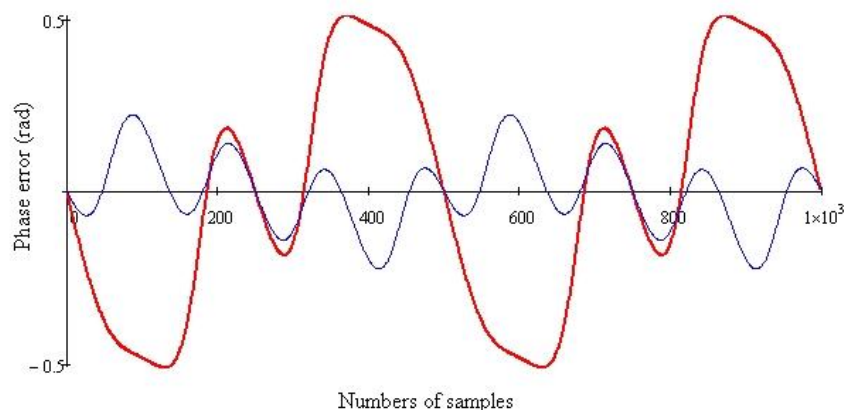


Fig. 6. The measurement error of phase due to distortion of the profile of interference fringes.

For the algorithm (4), the maximum absolute error of phase measurement was 0.512 rad., and for the algorithm (15) – 0.224 rad. The standard deviation (RMS) for the same algorithms was 0.055 and 0.017, respectively. Due to the special selection of phase shifts, the proposed algorithm (14) has errors at the level of sampling error of the original signal, i.e. it practically does not depend on the distortion of the interference fringes profile.

CONCLUSION

The algorithm of interferograms analysis (demodulation) in step-by-step phase shift methods is presented. The comparison of the proposed algorithm with the known algorithms, in particular, with multi-point algorithm (15). Due to the special selection of phase shifts, the proposed algorithm is resistant to interference fringe profile distortion in a wide range of gamma distortion coefficient values.

ACKNOWLEDGMENT

This work was supported by RFBR (grant № 18-08-00580)

REFERENCES

1. F.V. Bulygin, Optical and electronic measurements. Collection of articles, Edited by V.S. Ivanova, Moscow: Publishing office “University book”, 2005, p. 420.
2. V.I. Guzhov, S.P. Il'yinykh, R.A. Kuznetsov, D.S. Haydukov, “Generic algorithm of phase reconstruction in phase-shifting interferometry,” *Opt. Eng.* 2013, 52(3):030501
3. C.A. Poynton, “Gamma” and its disguises: The nonlinear mappings of intensity in perception, CRTs, film and video,” *SMPTE J.*, 1993, pp 1099:1108.
4. A. Siebert, “Retrieval of gamma corrected images,” *Pattern Recognition Letters* 22, 2001, pp. 249-256.
5. H. Farid, “Blind inverse gamma correction,” *IEEE Trans. Image Processing* 10, 2001, pp. 1428-1433.
6. S. Zhang and S. Yau, “Generic nonsinusoidal phase error correction for three-dimensional shape measurement using a digital video projector,” *Appl. Opt.* 2007, vol. 46, pp. 36-43.
7. V.I. Guzhov, S.P. Il'yinykh, I.A. Sazhin, E.N. Denezhkin, E.S. Kabak, and D. S. Khaidukov, “Quasiheterodyne method of interference measurements,” *Optoelectronics, Instrumentation and Data Processing.*, 2015, vol. 51, iss. 3, pp. 280-286.
8. V.I. Gushov, S.P. Il'yinykh, D.S. Haidukov, R.A. Kuznetsov, “Method of an Assessment of Reliability of High-Precision Measurements,” *Proceedings of APEIE 2012.* 11-

th International Conference on actual problem electronics instrument engineering. vol. I, pp. 105–106.

9. Guzhov V.I. Phase information recovery based on the methods of phase shifting interferometry with small angles between interfering beams / V.I. Guzhov, S.P. Il'Inykh, S.V. Khaibullin // Optoelectronics, Instrumentation and Data Processing. - 2017. - Vol. 53, iss. 3. - P. 288-293. - DOI: 10.3103/S875669901703013X

10. Eliminating the effect of non-linear distortion of profile fringes for structured illumination method / Guzhov V., Ilinykh S., Marchenko.I, Emelyanov V. // Proceedings of IFOST-2016. The 11th International forum on strategic technologies (IFOST 2016), June 1-3, Russia, Novosibirsk, 2016, Vol. 1, pp. 535–537.

11. D. Malacara, “Optical Shop Testing,” 3rd Edition, Wiley-Interscience, 2007, p.883.

AUTOMATION OF FATIGUE VIBRATION TESTING AT HIGH TEMPERATURES

Palaguta K.A., Lvov N.Yu, Lvovskiy T.A.
Moscow, Moscow Polytech University
+7 (909) 698-16-15, ka129@yandex.ru

Abstract The article deals with the issues offatigue vibration automation of tests at high temperatures. It is proposed to use a shadow optical sensor that allows you to work at high temperatures. The algorithm maintain resonance during the test.

Keywords: fatigue vibration tests; high temperatures; shadow optical sensor.

INTRODUCTION

Nowadays, the reliability of rotor blades in gas turbine power plants is a topical issue. It is from their design and technological features that gas-dynamic properties of engines and the reliability of their operation fundamentally depend. The conditions in which the blades operate during the operation of the turbine can be described as severe. Moreover, the resource of turbine blades determines the reliability and resource of the entire engine.

When the turbine is operated on an airplane or in an electric power plant, the main cause of vibration in the blades is the gas-air flow, the properties depend on the design of engine, its characteristics, conditions and operation mode.

Stand-tests on fatigue strength of blades are carried out on vibro-stands, which, depending on the design and operating principle, are divided into electrodynamic, hydraulic, mechanical, electromagnetic, piezoelectric, magnetostrictive, resonance and others [5]. Electrodynamic vibration units have been and remain the most common in industrial tests. Among their advantages, which has led to their widespread use, include the following:

- Wide range of reproducible frequencies of table movement (more than 2000 Hz);
- Ability to achieve high speeds and accelerations (acceleration value can reach 1000 m / s²);
- Great flexibility in choosing the form of the control signal.

There are a number of methods for the numerical analysis of stresses in the estimation of multicycle fatigue of GTE blades [4], each has a certain set of positive qualities.

At the same time, because in the process of working properties and characteristics of the blades changed as a result of changes of temperature and speed of rotor rotation, the results of the solution of forced vibrations are always an approximation.

STATEMENT